

THz calorimetry: an absolute power meter for TeraHertz radiation and the absorptivity of the Herschel Space Observatory telescope mirror coating

Tjeerd O. Klaassen^{*a}, J. Niels Hovenier^a, Jacqueline Fischer^b, Gerd Jakob^c, Albrecht Poglitsch^c and Oren Sternberg^b

^aFaculty of Applied Sciences, Delft University of Technology, P.O. Box 5046, 2600 GA Delft, The Netherlands;

^bNaval Research Laboratory, Remote Sensing Division, Code 7213, Washington, DC 20375, USA;

^cMax-Planck-Institute für Extraterrestrische Physik, Postfach 1603, D-85740, Garching, Germany

ABSTRACT

A new calorimetric absolute power meter has been developed for THz radiation. This broad band THz power meter measures average power at ambient temperature and pressure, does not use a window, and is insensitive to polarization and time structure of THz radiation. The operation of the power meter is based on the calorimetric method: in order to determine the power of a beam of THz radiation, the beam is used to illuminate a highly absorbing surface with known BRDF characteristics until a stable temperature is reached. The power in the incident beam can then be determined by measuring the electric power needed to cause the sample temperature rise. The new power meter was used with laser calorimetry to measure the absorptivity, and thus the emissivity, of aluminum-coated silicon carbide mirror samples produced during the coating qualification run of the Herschel Space Observatory telescope to be launched by the European Space Agency in 2007. The samples were measured at 77 Kelvin to simulate the operating temperature of the telescope in its planned orbit around the second Lagrangian point, L_2 , of the Earth-Sun system. The absorptivity of both clean and dust-contaminated samples was measured at 70, 118, 184 and 496 μm and found to be in the range 0.2 – 0.8%.

Keywords: Herschel Observatory, mirror absorptivity, TeraHertz radiation, TeraHertz power meter.

I. INTRODUCTION

For passively-cooled telescopes such as the European Space Agency's Herschel 3.5-meter silicon carbide telescope^{1,2} to be launched aboard an Ariane 5 rocket to orbit the Earth-Sun second Lagrangian point, L_2 , in 2007, the signal from the thermal self-emission of the Cassegrain telescope reflecting surfaces is expected to be the dominant source of noise for two of the three of the Observatory instruments. Thermal models of the telescope/spacecraft system predict an equilibrium operating telescope temperature of 70 – 90 K. Both the Photoconductor Array Camera & Spectrometer³ (PACS) and the Spectral and Photometric Imaging Receiver⁴ (SPIRE), together providing both imaging and moderate resolution ($\lambda/\Delta\lambda$ 100 - 2000) spectroscopy over the 55 – 670 μm spectral range, are expected to be background limited by the thermal self-emission of the telescope reflecting surfaces. In order to estimate the background flux on their detectors and the sensitivity of these instruments in orbit and to determine the degree to which stray light must be reduced, we have carried out a set of measurements designed to estimate the expected emissivity of the mirror surfaces in orbit in the sub-millimeter spectral range.

For opaque coatings, the reflectivity R is equal to $1 - \epsilon$, so that formally an alternative method to measure ϵ is to measure the reflectivity⁵, which is often an easier quantity to measure. However for coatings with high reflectivity and small absorptivity, say $R > 0.99$ and thus $\alpha < 0.01$, the required accuracy in the determination of R , on the order of 0.1%, is prohibitive. The emissivity of a surface can be measured by comparing its thermal emission to that of a reference surface⁶. However the lack of a suitable reference surface, and the need for special filters at each wavelength to

* t.o.klaassen@tnw.tudelft.nl; phone +31 15-2786136; fax +31 15-2788128

determine the emissivity, necessitates a different way to determine ϵ . Therefore we choose to measure the absorption coefficient α , employing a calorimetric method.

According to Kirchhoff's law⁷, for equilibrium conditions, the fraction of blackbody radiation emitted by the surface of an object at a given temperature and wavelength, its emissivity ϵ , is equal to the fraction it absorbs at the same temperature and wavelength, its absorptivity α . This applies to total, spectral, directional, and polarization quantities. So one can indirectly determine the emissivity of a surface measuring calorimetrically the fraction of radiation that it absorbs at a given wavelength.

For the calorimetric technique employed, an accurate determination of the wavelength dependent power of the THz laser source is needed. The lack of good power meters for the THz region triggered therefore also the development of a simple room temperature broadband absolute power meter, based on the same calorimetric technique.

II. TERAHERTZ CALORIMETRY

The calorimetric method to determine absorbed THz power, used in the experiment for the Herschel mirror samples as well as for the calibration of the absolute power meter, was developed earlier to determine the THz absorption losses of rough gold surfaces at low temperatures^{8,9,10}. The principle of the experiment is simple: the surface under investigation is weakly coupled to a thermal bath and then illuminated by FIR-radiation of known wavelength and power P_0 , until a stable sample temperature is reached. The resulting small temperature increase ΔT is recorded through a temperature sensor, which is glued to the backside of the sample. $\Delta T = P_{\text{abs}}/G$, with P_{abs} the optical power absorbed per second and G the heat flow from the sensor towards the surrounding, which is supposed to be at a constant temperature. The thermal time constant τ with which the sensor temperature reaches an equilibrium value is given by $\tau = C/G$, with C (J/K) the heat capacity of the sensor. Subsequently, the far-IR radiation is blocked and the sample is electrically heated via a resistor, which is also glued to the backside of the sample. The heating current is then adjusted until the sample reaches equilibrium at the same temperature that was recorded during laser illumination, thereby heating the sample with power $P_{\text{el}}=I_{\text{H}}V_{\text{H}}$, where I_{H} and V_{H} are the heater current and voltage respectively. As long as the heat conductivity of the sample substrate is high, the heat is quickly distributed across the sample and thus the electrical and radiative heat input to reach the same reading of the temperature sensor are equal, i.e. the electrical heating power P_{el} is equal to the absorbed FIR-power P_{abs} .

For the experiments on the *mirror coating* samples, the incoming THz power P_0 is known, and the absorptivity α , and thus the emissivity ϵ , at a given laser wavelength can be derived from:

$$\epsilon = \alpha = P_{\text{abs}}/P_0 = P_{\text{el}}/P_0 .$$

For the experiments with the *absolute power meter*, the absorption coefficient α of the now *highly absorbing* sensor surface can be determined accurately from reflection (BRDF) experiments (see later). The absolute power P_0 of a THz beam can then be determined by such a calorimetric experiment from:

$$P_0 = P_{\text{el}}/\alpha$$

III. THZ POWER METER

3.1 Introduction

Essential for the determination of the wavelength dependent absorption coefficient of the mirror coating is the ability to measure the THz power accurately. This however is a big problem, largely due to the fact that many materials that are good optical absorbers in the visible or near- and mid-infrared region show a rapidly increasing reflectivity and decreasing absorptivity towards the far infrared. For relatively weak THz sources the power is sometimes determined by using a liquid Helium cooled Si bolometer, comparing the signal induced by the source with that induced by a black body radiation source of known dimensions and temperature. However, for such a determination to be accurate, a good knowledge of the wavelength dependent emissivity of that black body source is needed. In general, quantitative data on this strong increase in reflectivity and decrease in absorptivity/emissivity of most materials towards longer wavelengths are not available.

Prior to this work, the only reliable power meter for THz radiation known to us was the "TK Terahertz Absolute Power Meter System" (Thomas Keating Ltd.). Its working is based on the principle that a "free standing" thin metal film with a

sheet resistance $R_{\square} = 60\pi \Omega$, i.e. one half of the vacuum impedance $Z_0 = 120\pi \Omega$, will absorb exactly one half of the optical power incident on its surface. (It must be noted that this holds only as long as the frequency of the optical wave is below the plasma frequency of the metal film). In this power meter the thin metal film is evaporated on a polythene membrane, placed inside a Golay cell. The absorbed optical power is determined by comparing the signal under optical illumination with that resulting from electrical heating of the same metal film. To employ this instrument properly, the THz source should have a square wave modulated intensity with a repetition frequency preferably of the order of 30 Hz. To eliminate the wavelength dependent etalon effects in the entrance window of the Golay cell, the source beam has to be linearly polarised and applied under Brewster's angle. Moreover, the entrance window exhibits a wavelength dependent absorption. To avoid this type of restrictions/problems, we developed and constructed a simple broadband power meter, based on the same calorimetric principle as used for the mirror absorptivity measurements. This instrument puts no restrictions on shape, polarisation or temporal behaviour of the incoming beam. The power meter is used at ambient temperature, without entrance window. The power sensor consists of an aluminium substrate, on the front side covered with a rough broad band THz absorbing coating, and a temperature sensor and a heater resistor on the back side.

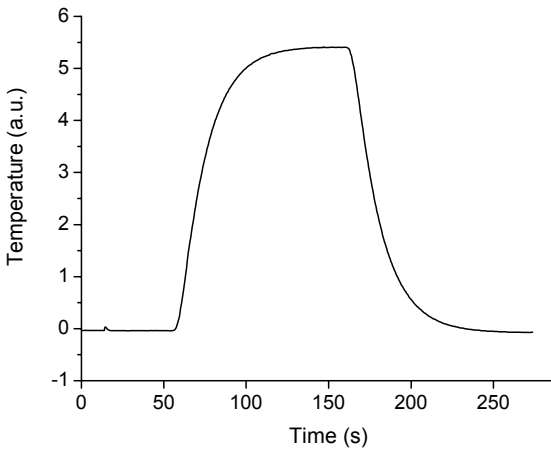


Fig. 1. Thermal response of the absolute power meter sensor

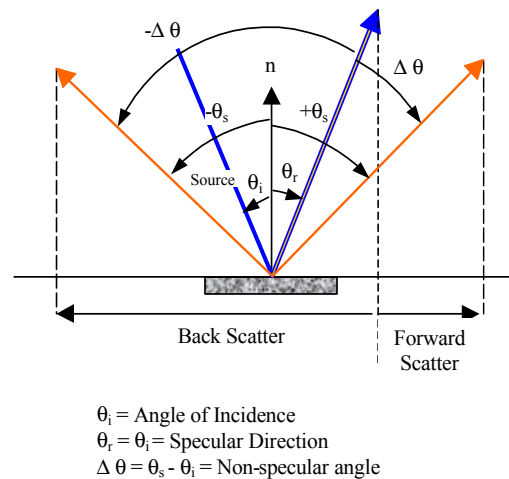


Fig. 2. Definition of scattering configuration. All directions indicated are in the optical plane, defined by the surface normal \mathbf{n} and the incoming beam.

As mentioned before, most black surfaces that are very good absorbers at short wavelengths, appear to become more or less reflecting for wavelengths in the far infrared region. From earlier work on the development of THz absorbing surfaces, we know that the crucial step towards efficient absorption for this wavelength region is the use of a *rough* absorbing surface. In fact, the surface roughness should be of the order of the wavelength in order to suppress specular reflection properly. The wavelength dependent absorption coefficient $\alpha(\lambda)$ equals $1 - \text{THR}(\lambda)$, with $\text{THR}(\lambda)$ the wavelength dependent Total Hemispherical Reflection. This quantity can be determined accurately by measuring the Bi-directional Reflection Distribution Function (BRDF) as a function of the angles of incidence and reflection of the radiation as a function of wavelength¹⁰.

3.2 Design

The sensor head consists of a 1 mm thick, 25 mm diameter circular aluminium substrate with on the front side a broad band THz absorbing coating. At the backside a 100 Ω Pt resistor to monitor the temperature and a 470 Ω electrical heater have been attached. This substrate is connected with an aluminium rod to a big brass block that serves as the constant temperature bath. The rod dimensions are such that a (1/e) thermal time constant of $\tau \approx 20$ sec is obtained, see Fig. 1. The temperature increase of the absorber under optical or electrical heating is measured by comparing the resistance of the Pt-100 sensor on the backside of the absorber with that of a Pt-100 sensor attached to the constant temperature bath, using an AC Wheatstone bridge circuit with phase sensitive lock-in detection. Temperature differences of less than 0.5 mK's can be measured easily that way. The minimum average power that can be measured at present, with this not yet optimised system, is about 10^{-4} W.

For the absorbing surface some of the coatings that we developed earlier as broadband THz absorbers for the HIFI spectrometer aboard the Herschel platform have been considered⁸⁻¹¹. These coatings are fabricated for HIFI on aluminum substrates too. After a careful preparation of the surface, a thin layer of Stycast 2850 FT + 24 LV Catalyst is applied and subsequently a mixture of Stycast and SiC grains. For the power meter under consideration a SiC grain size of 500 μm has been used. Also commercially available SiC "open foam" materials with 60 ppi (pores per inch) and a density of 12% (ERG Materials and Aerospace Corp., Oakland, CA, USA) can be used as absorber. These foams exhibit a good heat conductivity together with a low heat capacity. To enhance the absorptivity, the foam can be coated with an additional thin layer of Stycast 2850 FT.

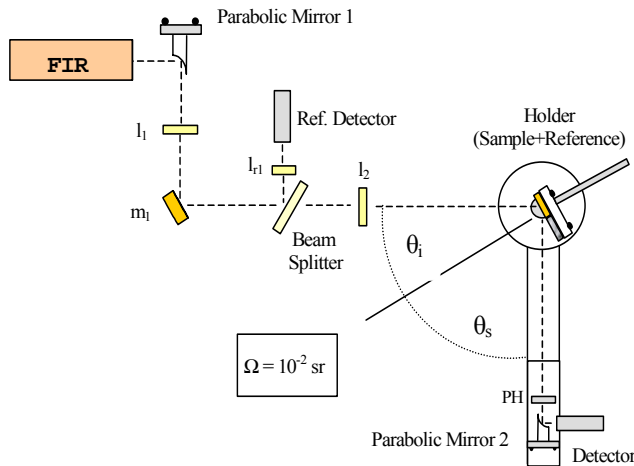


Fig. 3. Experimental set-up for the BRDF measurements.

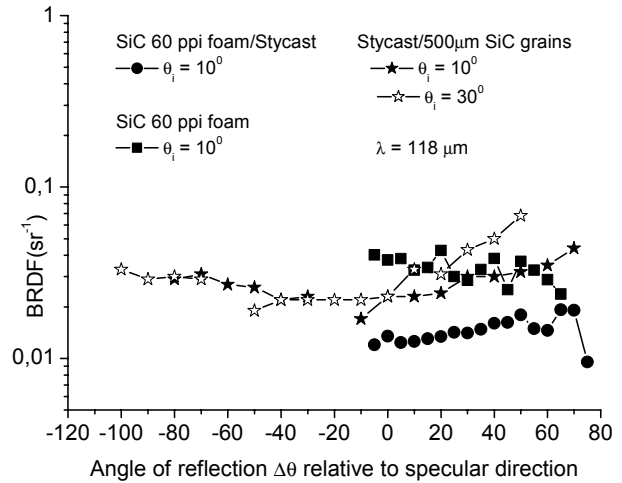


Fig.4. BRDF for 3 different coatings for $\lambda = 118 \mu\text{m}$

3.3 Determination of the sensor absorptivity

The Bi-directional Reflectance Distribution Function (*BRDF*) is the proper quantity to describe the (diffuse) reflection properties of rough surfaces. It is defined as the reflectance per unit projected detector solid angle as a function of the azimuthal coordinates θ and ϕ and given in units of inverse steradians (sr^{-1}). Usually it is measured in the plane of incidence, defined by the incoming optical beam and the surface normal (i.e. $\phi=180^\circ$), versus the non-specular angle $\Delta\theta$ (see Fig.2 for the definition of the various angles).

$$BRDF(\Delta\theta, \lambda, \theta_i) = \frac{P_s(\Delta\theta, \lambda, \theta_i)}{P_o(\lambda, \theta_i) \Omega \cos\theta_s}$$

Here P_s is the power, diffusely scattered by the surface, in the direction θ_s within the solid angle Ω . P_o is optical power of the parallel beam of radiation directed at the sample under an angle θ_i with the surface normal. The factor $\Omega \cos\theta_s$ is the projected detector solid angle. For a non-absorbing perfect diffuse scatterer, a so-called Lambertian surface, the BRDF is independent of direction and equals π^{-1} . In general the system is set up such as to monitor the scattered radiation within a solid angle $\Omega \approx 0.01 \text{ sr}^{-1}$.

The optical properties of the coatings have been studied using monochromatic light at wavelengths of 70 μm , 118 μm , 184 μm , 335 μm and 496 μm , created by a standard optically pumped far-infrared laser.

Measurements of the BRDF for a number of directions of incident light ($0^\circ \leq \theta_i \leq +30^\circ$) have been carried out, in order to cover the conditions met for a slightly focussed or divergent beam hitting the sensor. The influence of variations in shape and intensity of the laser beam has been eliminated by comparing all samples with a reference sample consisting of a gold-coated rough surface, acting as a near Lambertian reflector, accurately calibrated against the total reflection of a gold-coated mirror. The near parallel Gaussian-like THz beam is shaped such that the waist (with a $1/e^2$ diameter ≈ 10 mm) is situated at the sample surface to assure a well-defined angle of incidence of the light. The scattered light is detected with a 2 mm diameter room temperature pyroelectric detector (Eltec) with home made sensitive read-out electronics¹². The schematic experimental setup is shown in Fig. 3.

The scattering characteristics (BRDF) of some of the surfaces studied are presented in Fig.'s 4 –7. For the calibration of the Scientec power meter used in the mirror experiments, a Stycast/500 μm SiC grain surface was used.

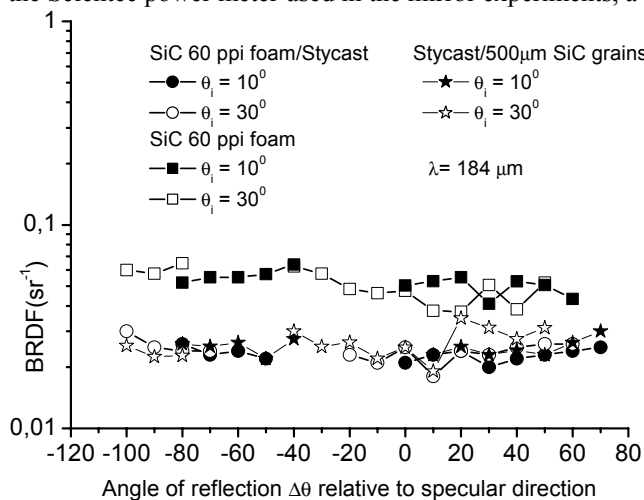


Fig. 5. BRDF for 3 different coatings for $\lambda = 184 \mu\text{m}$

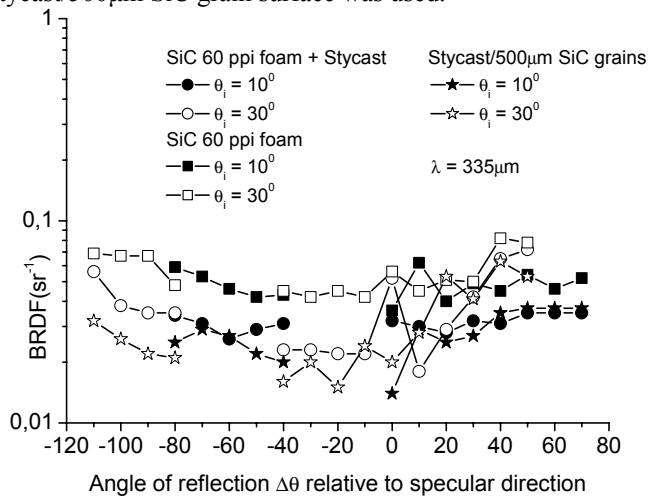


Fig. 6. BRDF for 3 different coatings for $\lambda = 335 \mu\text{m}$

The “scatter” in the angular dependence of the experimental BRDF data is the result of a non-perfect random rough surface, leading to a directional dependence of the diffuse scattering. The observed increase of the scattering near $\theta_i = 0$, the specular direction, that shows up at longer wavelengths, is not such an artifact, but reflects the actually increased reflection because the roughness of the surface is not anymore larger than the wavelength of the radiation.

The directionally averaged values of the BRDF of the well absorbing surfaces (SiC 60 pp foam with Stycast coating and the Stycast with 500 μm SiC grains) fall in the range of $0.02 - 0.04 \text{ sr}^{-1}$. Consequently, the THR ranges from 6.5 to 13 % and thus the overall absorption is 93.5 – 87 %. Because of this large absorption value the *relative* error in the value of the absorption is about 9 times smaller than the *relative* error in the value of the BRDF.

Using the actual BRDF data for a surface, the wavelength dependent total absorption for illumination with light with an angle of incidence $\theta_i \leq 30^\circ$ is easily calculated. It should be noted that, because the BRDF gives the reflected light per steradian, an increase of its value for a specific direction, notably in the specular direction $\theta_i = 0$, does not need to influence strongly the value of the overall absorption.

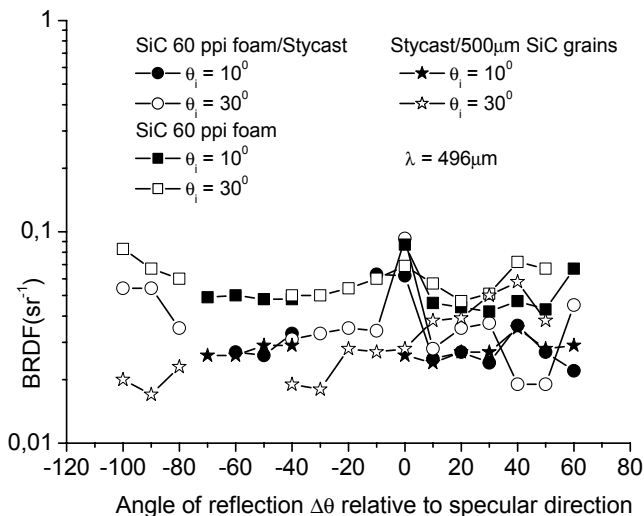


Fig. 7. BRDF for 3 different coatings for $\lambda = 496 \mu\text{m}$

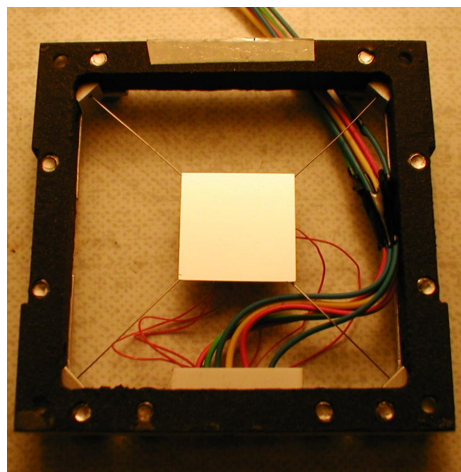


Fig. 8. Photograph of a sample and sample carrier

IV. HERSCHEL MIRROR EXPERIMENTS.

4.1 Sample preparation

In order to most accurately represent the Herschel Space Observatory telescope, the sample substrates were made of silicon carbide, prepared and polished with the same surface roughness as the Herschel telescope (< 30 nm rms) by Opteon Ltd. (Finland) for EADS-Astrium (France). The samples were cut and ground to dimensions $14\text{ mm} \times 14\text{ mm} \times 0.5\text{ mm}$ in order to minimize their heat capacity while insuring that the beam could be focused onto the sample. The samples were coated with aluminum and a thin protective layer of *Plasil*, a form of SiO_2 developed by Leybold Optics (Germany), during the qualification Herschel mirror coating run at Calar Alto Astronomical Observatory in Spain. Since they were placed at different positions in the coating chamber they had different thicknesses, d , of the coating layers. Measurements were done on the two samples with the largest thickness differences. For Sample 1, $d(\text{aluminum}) = 400$ nm, $d(\text{Plasil}) = 25$ nm, and for Sample 2, $d(\text{aluminum}) = 300$ nm, $d(\text{Plasil}) = 7$ nm. A third set of measurements was done on Sample 2 after contamination with dust at a level of 5000 ± 50 areal parts per million (ppm)¹³. Prior to contamination the clean samples were inspected with bright illumination and microscope cleanliness and particle counting tests were performed. The samples were found to be free from gross defects with minimal contamination and no particles larger than 5 microns were observed. Dust for the contamination was collected from a class 100.000 clean room at the European Space Research and Technology Center (ESTEC) Test Center. This type of dust was chosen to represent what might fall on the Herschel telescope from the Ariane rocket fairing during storage. The dust was deposited on the sample and adjusted to 5000 ppm with a soft helium gas flow. The particle count was rechecked after vertically positioning the sample in a vacuum chamber at 10^{-6} mbar pressure and again after completion of the absorptivity measurements in the cryostat. Particle count and size measurements were carried out at six positions, and were found to be similar, before and after the absorptivity measurements.

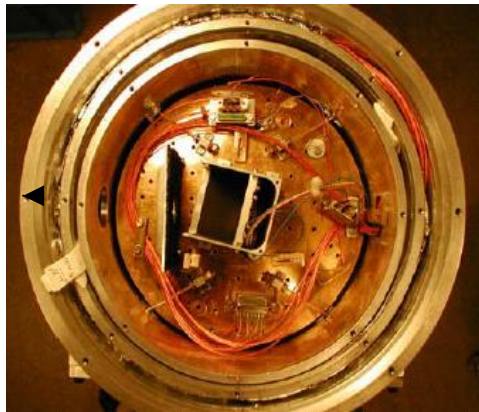


Fig. 9. Cryostat cold-plate and sample housing. The laser beam enters through the cryostat window at the left, passes through the aperture in the absorbing screen, and is reflected by the tilted sample back onto the absorbing screen.

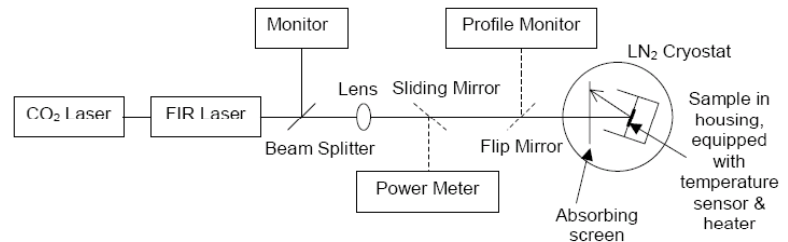


Fig. 10. Schematic drawing of the optical configuration used for the measurements. Sliding and flip mirrors are inserted into the beam for power calibration and beam profile verification, respectively.

4.2 Sample housing and thermal connection to the 77 K bath

Since the passively cooled Herschel telescope operating temperature is expected to be in the 70–90 K range, the samples were mounted in a sample housing on the cold-plate of a dewar filled with liquid nitrogen, i.e. at 77 K. Figure 8 is a photograph of the sample carrier in the sample housing. The sample carrier and the inner surfaces of the box were coated with black paint and the wires and electrical connections to the sample were baffled by aluminum tape (not shown in Fig. 8). The samples are held by 4 steel wires of 200 μm diameter with a length of about 23 mm, which are attached with screws to the rectangular carrier. The carrier is screwed to the box and the sample box is directly screwed to the 77 K cold plate of the cryostat (Fig. 9). The choice of the exact value of the chosen thermal coupling G of the sample to the 77 K bath was a trade-off between the desire to reach a large temperature increase and a small thermal time constant.

The thermal time constant $\tau = C / G$, where C is the heat capacity of the sample, while the temperature increase $\Delta T \propto P_{\text{abs}} / G$. The electrical connection of the heater (2 wires) and the temperature sensor (4 wires) was accomplished with 6 constantan wires of a diameter of $75 \mu\text{m}$ and a length of $\sim 40 \text{ mm}$. These parameters were chosen to yield a thermal time constant of minutes and such that the contribution of the constantan wires to the thermal coupling would be small compared to that of the 4 steel wires. Experimentally we found that the thermal time constant τ was of order 10 minutes see Fig. 12), over which the laser was stable, and the temperature increase ΔT large enough ($\geq 0.1 \text{ K}$) to be easily measured with the AC Wheatstone bridge circuit.

4.3. Experimental details

The measurements were performed with an Edinburgh Instruments Ltd Model 295 CO₂-pumped far-IR laser. In order to cover most of the spectral range of the Herschel Space Observatory suite of instruments, four strong lines were chosen for the measurements: the $70 \mu\text{m}$ and $118 \mu\text{m}$ lines of CH₃OH (Methanol), the $184 \mu\text{m}$ line of CH₂F₂, and the $496 \mu\text{m}$ line of CH₃F. Figure 10 is a schematic drawing of the optical set-up of the far-IR laser absorption measurements and Figures 9 and 11 are photographs of the cryostat cold plate and the optical setup. A $12 \mu\text{m}$ thick Mylar beam-splitter reflects a small fraction of the laser power to a pyroelectric monitor to record any change of the incoming laser power. A polyethylene lens focuses the laser beam through the polyethylene cryostat window onto the sample, which is tilted at an angle of 14 degrees with respect to the laser beam. This configuration directs the reflected beam onto an absorptive screen, located in front of the cryostat window, consisting of an aluminum substrate coated with an absorptive mixture of 1-mm silicon carbide grains and black Stycast 2850 FT. This screen absorbs 95% of the radiation reflected from the sample. To absorb radiation spilling over the edge of the sample, an identical absorbing screen is mounted to the rear wall of the sample housing. A flip-mirror in front of the cryostat was used to be able to monitor the position and beam profile of the focused beam at the sample position with a second pyroelectric detector located at the same distance from the lens as the sample. Horizontal and vertical $1/e^2$ beam diameters measured with the monitor are in the range of 6 – 7. mm at wavelengths of $70, 118,$ and $184 \mu\text{m}$, and about 12 mm at $496 \mu\text{m}$. Before and after the far-IR irradiation of the sample, a slide-in mirror, also in front of the cryostat window, is used to direct the light to a Scientech 380101 UV/NIR volume absorbing calorimeter interfaced to a Scientech 372 power meter used to monitor and record the laser power level incident on the window of the cryostat. The calibration of this power meter at the laser line wavelengths in question has been performed with the absolute power meter described above.

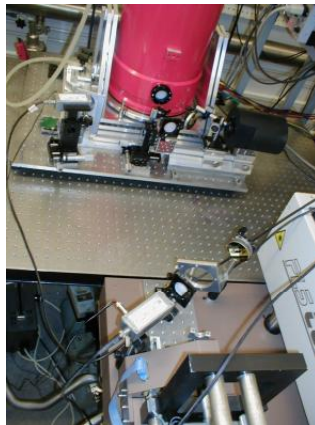


Fig. 11. View of the experimental set up, with the FIR laser exit below and the dewar with beam shaping and monitoring optics.

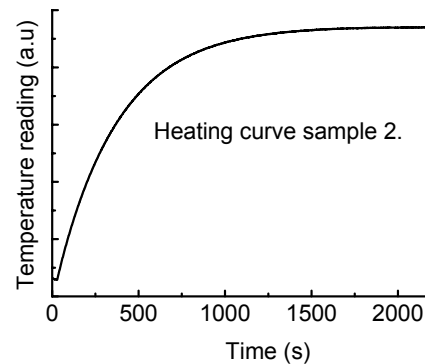


Fig. 12. A typical heating curve of a mirror sample at $T = 77 \text{ K}$. $\Delta T \approx 300 \text{ mK}$, noise level $\approx 0.6 \text{ mK (rms)}$, $\tau \approx 7 \text{ minutes}$.

The temperature increase of the sample resulting from either far-IR illumination or electrical heating with a 470Ω thin film resistor is measured with a Pt-1000 temperature sensor at the backside of the sample. A Pt-1000 temperature sensor is mounted on the sample housing, which is in good thermal contact with the cryostat cold plate and assumed to be at constant temperature, acts as the references resistor for the AC Wheatstone bridge used to measure the temperature of the

sample. This method provided an rms noise level of about 0.6 mK, providing a significant improvement in signal-to-noise compared with a 4-point direct resistance measurement used in an earlier calorimetric experiment⁹. An example of a typical heating curve is shown in Figure 12.

4.4 Measurements and results

Measurements of the heater power that produced the same temperature increase as the laser power absorbed by the mirror and of the power measured by the Scientech power meter were taken with the beam centered on the sample. To ensure that this value was representative, a number of measurements were taken for beam positions around the sample center. The position of the beam was varied by moving the focusing lens in transverse directions and monitored using the second pyroelectric detector.

The absorptivity values and their uncertainties are presented in Table 1. They are based on the weighted mean values of the ratio of the electrical heating power, P_H , to the power reading on the Scientech power meter, measured at a small number of positions in the central region of the samples. It must be noted that the actual optical power reaching the sample was deduced from the Scientec readings taking into account the proper wavelength dependent calibration and correcting for absorption of the polythene window of the dewar. Also the effect of small differences in path length through air for the beam directed to the sample and to the power meter respectively, leading to differences in power attenuation as a result of absorption by water vapor, has been taken into account.

The uncertainties quoted in the table are based on a conservative consideration of all possible errors, including all steps leading to the Scientec calibration, uncertainties in water vapor absorption and the effects of stray light inside the dewar, absorbed by the – highly absorbing – backside of the mirror samples. For the shorter wavelengths (70, 118, and 184 μm), where the sample was illuminated with a beam with narrow waist, this error is estimated to be $\pm 25\%$. At 496 μm , the larger size of the beam diameter is thought to lead to a small amount of spillage of the laser power over the edge of the sample, with subsequent scattering leading to non-negligible absorption on the back side of the sample, and consequently systematic errors in the absorption coefficient at 496 μm are estimated to be +25% and –50%.

Sample	$\lambda =$	70 μm	118 μm	184 μm	496 μm
1. 300 nm Al + 7 nm Plasil		0.31	0.32	0.27	0.33
		(± 0.08)	(± 0.08)	(± 0.07)	($\pm 0.08/0.17$)
2. 400 nm Al + 25 nm Plasil		0.39	0.32	0.28	0.36
		(± 0.10)	(± 0.08)	(± 0.07)	($\pm 0.09/0.18$)
Sample 2. with 5000 ppm dust		0.79	0.54	0.39	0.23
		(± 0.20)	(± 0.14)	(± 0.10)	($\pm 0.06/0.12$)

Table 1. Absorptivity (%) of the three measured samples at $T = 77\text{ K}$

There is no statistically significant difference between the measured values of the two clean samples, despite their differing thicknesses of aluminum and Plasil layers. Since the skin depth of aluminum at 77 K is more than an order of magnitude smaller than the aluminum layer thickness of both samples, no laser radiation is expected to reach the SiC substrate for either sample. Thus the similarity in the absorptivity of both clean samples suggests that the absorption in the Plasil layer is less than our measurement uncertainties, i.e. $< 0.10\%$. In order to check for a strong temperature dependence of the emissivity in this temperature range, one measurement at each wavelength was taken at 66 K while pumping on the liquid nitrogen bath for samples 1 and 2. No statistically significant differences were observed.

The measured values are 0.1 – 0.2% higher than the absorptivity expected for a pure aluminum mirror based on the Hagen and Rubens formula¹⁴ and the DC resistivity of aluminum¹⁵ at 77 K ($0.23 \cdot 10^{-8} \Omega \text{ m}$).

Discrepancies could possibly be attributed to surface roughness and surface preparation issues and to the complex and frequency dependent nature of a metal's resistivity¹⁶. In particular, we have investigated the importance of small holes observed to be present on the surface of the Herschel mirrors (100 holes/mm², radii $\sim 2 \mu\text{m}$) due to the preparation of the SiC substrate, using electromagnetic field simulation software and found no significant effect due to the presence of the holes.

In contrast with the clean samples, the dusted sample shows a clear increase of absorption with decreasing wavelength, as could be expected for wavelengths greater than the dust particle size is expected¹⁷.

ACKNOWLEDGEMENTS

We gratefully acknowledge suggestions made by the Herschel Project Scientist Göran Pilbratt and by Pierre Olivier (ESA/ESTEC), mirror samples supplied by Dominique Pierrot (EADS-Astrium, France), and sample contamination and characterization by Olivier Schmeitzky and Mark van Eesbeck (ESA/ESTEC). We also thank Thomas Passvogel and Daniel de Chambure for making available partial funding of these measurements from the European Space Agency Herschel/Planck Project Office. JF and OS acknowledge support from the Office of Naval Research and the National Aeronautics and Space Administration's Herschel Project Office at the Jet Propulsion Laboratory.

REFERENCES

1. E. Sein, Y. Toulemon, F. Safa, M. Duran, P. Deny, D. de Chambure, T. Passvogel, and G. Pilbratt, "A Φ 3.5 M SiC telescope for Herschel mission", *Proc. IR Space Telescopes and Instruments*, J. Mather, ed., SPIE **4850**, 606-618 (2003.)
2. G. Pilbratt, "Herschel Space Observatory mission overview", *Proc. IR Space Telescopes and Instruments*, J. Mather, ed., SPIE **4850**, 586-597 (2003).
3. A. Poglitsch, C. Waelkens, and N. Geis, "The Photoconductor and Array Camera & Spectrometer (PACS) for the Herschel Space Observatory", *Proc. IR Space Telescopes and Instruments*, J. Mather, ed., SPIE **4850**, 662-673 (2003).
4. M. Griffin, B. Swinyard, and L. Vigroux, "SPIRE – Herschel's Submillimetre Camera and Spectrometer", *Proc. IR Space Telescopes and Instruments*, J. Mather, ed., SPIE **4850**, 686-696 (2003).
5. J.J Bock, M.K. Parikh, M.L. Fischer and A.E. Lange, "Emissivity measurements of reflective surfaces at near-millimeter wavelengths", *Appl. Opt.* **34**, 4812-4816 (1995).
6. A.J. Gatesman, R.H. Giles and J. Waldman, "High-Precision reflectometer for submillimeter wavelengths", *J. Opt. Soc. Am. B* **12**, 212-219 (1995).
7. W. L Wolfe, *Radiation Theory, in The Infrared & Electro-Optical Systems Handbook*, Accetta, D. L., Shumaker, D.L. eds., Volume 1: Sources of Radiation Zissis, G. J. ed., (ERIM, Infrared Information Analysis Center, Ann Arbor, Michigan & SPIE Optical Engineering Press, Bellingham, Washington, 1993), pp. 3-32.
8. T.O. Klaassen, J.H. Blok, N.J. Hovenier, G. Jakob, D. Rosenthal, K.J. Wildeman, "Absorbing coatings and diffuse reflectors for the Herschel platform sub-millimeter spectrometers HIFI and PACS", *Proc. 2002 IEEE Tenth International Conference on Terahertz Electronics* (Eds. J.M. Chamberlain, A.G. Davies, P. Harrison, E.H. Linfield, R.E. Miles and S. Withington) IEEE Catalog Number 02EX621, 32-35 (2002.).
9. T.O. Klaassen, J.H. Blok, J.N. Hovenier, G. Jakob, D. Rosenthal, K.J. Wildeman, "Scattering of sub-millimeter radiation from rough surfaces: absorbers and diffuse reflectors for HIFI and PACS", *Proc. IR Space Telescopes and Instruments*, J. Mather, ed., SPIE **4850**, 788-96 (2003).
10. M.C. Diez, T.O. Klaassen, C. Smorenburg, V. Kirschner, K.J. Wildeman, "Reflectance measurements on sub-millimeter absorbing coatings for HIFI", *Proc. Astronomical Telescopes and Instrumentation*, SPIE **4013** 129-139 (1999)
11. T.O. Klaassen, M.C. Diez, J.H. Blok, C. Smorenburg, K.J. Wildeman, G. Jakob, "Optical characterization of absorbing coatings for sub-millimetre radiation", *Proc. 12th International Symposium on Space Terahertz Technology*, JPL Publication 01-18, 400-409 (2001)
12. R.N. Schouten, "A new amplifier design for fast low-noise far-infrared detectors using a pyroelectric element", *Meas. Sci. Technol.* **9**, 686-91 (1998).
13. O. Schmeitzky, "Particle contamination simulation on SCI-sample-wafer Herschel-Planck project", ESTEC internal report TOS-QMC 2003/134, (2003).
14. M. Born and E. Wolf, *Principles of Optics*, Sixth Edition (Pergamon Press, Oxford, 1986).
15. G. W. C. Kaye and T. H. Laby, *Tables of Physical and Chemical Constants*, 16th Edition (Longman, Essex, 1995)
16. A. J. Gatesman, R. H. Giles and J.A. Waldman, "High Precision Reflectometer for Submillimeter Wavelengths", *J. Opt. Soc. Am. B* **12**, 212-219 (1995).
17. B. T. Draine and H. M. Lee, "Optical properties of interstellar graphite and silicate grains", *Astrophys. J.* **285**, 89 (1984).